VARIOUS METHODS OF RECONSTRUCTION
OF A CAVITY IN AN ORTHOTROPIC LAYER

A. O. Vatul'yan and O. A. Belyak

UDC 539.3

Direct and inverse problems of oscillations of an anisotropic layer with a cylindrical cavity of an arbitrary cross-sectional shape under the action of a load applied to the layer surface are considered. An asymptotic approach to solving these problems with cavities of small relative sizes is proposed. Numerical results of solving direct and inverse problems are presented.

Key words: *oscillations of semi-bounded solids with cavities, asymptotic, boundary integral equations.*

Introduction. Problems of oscillations of semi-bounded elastic solids with defects of different nature (cavities, inclusions, or cracks) compose an important class of dynamic problems of the elasticity theory. One of the most effective methods of solving the problems of the elasticity theory for areas with defects is reduction of the initial problems to systems of boundary integral equations with the use of the Green functions, which allows the dimension of the examined problem to be reduced by unity. Based on solving such problems, the wave fields in the layer can be calculated.

From the mathematical viewpoint, determining defects in an elastic medium on the basis of the measured field of displacements on the solid boundary is a rather complicated and little studied inverse geometric problem [1–4]. Various approaches are used to solve this problem. In the present work, we use an approach based on determining the characteristics of the wave field in a waveguide with a defect by various methods.

Formulation of the Problem. We consider steady oscillations (with a frequency ω) of an orthotropic elastic layer of thickness h with a cylindrical cavity, which does not reach the layer boundaries. The guide line of this cavity is a smooth closed curve l_0 with the generatrix parallel to the Ox_2 axis. The lower edge of the layer is rigidly fixed and coincides with the Ox_1 axis. The Ox_3 axis is directed vertically upward. The axes of elastic symmetry of the orthotropic material coincide with the coordinate axes. The oscillations in the layer are induced by a load $p_i(x_1)$ ($i = 1, 2, 3$) applied to the upper boundary of the layer.

After separation of the time factor, the boundary problem acquires the form

$$\sigma_{ij,j} + \rho\omega^2 u_i = 0; \tag{1}$$

$$u_i\Big|_{x_3=0} = 0, \quad \sigma_{i3}\Big|_{x_3=h} = p_i, \quad \sigma_{ij}n_j\Big|_{l_0} = 0, \quad \sigma_{ij} = C_{ijkl}u_{k,l}, \quad i,j = 1,2,3. \tag{2}$$

Here ρ is the density of the medium, C_{ijkl} are the components of the tensor of elastic constants of the material, which satisfy the known conditions of symmetry and the condition of positive determinacy, and n_j are the components of the unit vector of the normal to the curve l_0, which is external to the region occupied by the elastic medium. The problem formulation is closed by the conditions of wave radiation at infinity, with the principle of ultimate absorption being used in formulating these conditions [5].

Depending on the method of load application, the initial problem (1), (2) decomposes into two problems. Problem No. 1 is a problem of antiplane oscillations of the orthotropic layer with the cylindrical cavity [the component that differs from zero is $u_2(x_1, x_3)$; $i = 2$ and $j = 1, 3$ in the boundary problem (1), (2)]. Problem No. 2 is a

plane problem on oscillations of the layer with the cavity [the components that differ from zero are $u_1(x_1, x_3)$ and $u_3(x_1, x_3)$; $i, j = 1, 3$ in the boundary problem (1), (2)].

Solution of Direct Problems. The main method of studying the boundary problem (1), (2) is its preliminary reduction to an integral equation with an irregular kernel with the use of the potential theory [6–11]. Solutions of direct problems are constructed with the use of the Green functions for the layer $U_i^{(m)}(\boldsymbol{x}, \boldsymbol{\xi})$ ($i, m = 1, 2, 3$) and the generalized reciprocity theorem [12]. The Green functions [6, 12] for the layer are presented in the form of a single integral over the contour σ in the complex plane and have a logarithmic singularity at the origin.

In Problem No. 1, the displacement field in the layer under the action of the surface tangent load with a support on the segment $[a, b]$ is presented as

$$u_2(\boldsymbol{\xi}) = u_2^*(\boldsymbol{\xi}) - \int_{l_0} \sigma_{2j}^{(2)}(\boldsymbol{x}, \boldsymbol{\xi}) n_j(\boldsymbol{x}) u_2(\boldsymbol{x}) \, dl_x, \qquad j = 1, 3, \qquad u_2^*(\boldsymbol{\xi}) = \int_a^b p_2(x_1) U_2^{(2)}(x_1, h, \boldsymbol{\xi}) \, dx_1, \qquad (3)$$

and the integrand can be presented in the form

$$K(\boldsymbol{x}, \boldsymbol{\xi}) = \sigma_{2j}^{(2)}(\boldsymbol{x}, \boldsymbol{\xi}) n_j(\boldsymbol{x}) = \frac{1}{4\pi} \int_\sigma \frac{e^{i\alpha_1(x_1 - \xi_1)}}{\lambda} \Big(g_1(\alpha_1, \boldsymbol{x}, \xi_3) e^{-\lambda|x_3 - \xi_3|}$$

$$+ \frac{g_2(\alpha_1, \boldsymbol{x}) \sinh(\lambda \xi_3) e^{\lambda(x_3 - h)} - g_3(\alpha_1, \boldsymbol{x}) \cosh(\lambda(h - \xi_3)) e^{-\lambda x_3}}{\cosh(\lambda h)} \Big) \, d\alpha_1, \qquad (4)$$

where

$$g_1(\alpha_1, \boldsymbol{x}, \xi_3) = i\nu n_1(\boldsymbol{x})\alpha_1 - \text{sign}(x_3 - \xi_3)\lambda n_3(\boldsymbol{x}),$$

$$g_2(\alpha_1, \boldsymbol{x}) = i\nu n_1(\boldsymbol{x})\alpha_1 + \lambda n_3(\boldsymbol{x}), \qquad g_3(\alpha_1, \boldsymbol{x}) = i\nu n_1(\boldsymbol{x})\alpha_1 - \lambda n_3(\boldsymbol{x}),$$

$$\lambda^2 = \nu \alpha_1^2 - k^2, \qquad \nu = C_{66}/C_{44}, \qquad k^2 = \rho\omega^2/C_{44}.$$

In the case of plane strains (Problem No. 2), the wave fields in the layer under the action of the normal load applied to the segment $[a, b]$ of the layer surface $x_3 = h$ have the form

$$u_m(\boldsymbol{\xi}) = u_m^*(\boldsymbol{\xi}) - \int_{l_0} \Big[P_{m1}(\boldsymbol{x}, \boldsymbol{\xi}) u_1(\boldsymbol{x}) + P_{m3}(\boldsymbol{x}, \boldsymbol{\xi}) u_3(\boldsymbol{x}) \Big] \, dl_x, \qquad m = 1, 3, \qquad (5)$$

where

$$u_m^*(\boldsymbol{\xi}) = \int_a^b p_3(x_1) U_3^{(m)}(x_1, h, \boldsymbol{\xi}) \, dx_1,$$

$$P_{mk}(\boldsymbol{x}, \boldsymbol{\xi}) = \sigma_{1k}^{(m)}(\boldsymbol{x}, \boldsymbol{\xi}) n_1(\boldsymbol{x}) + \sigma_{3k}^{(m)}(\boldsymbol{x}, \boldsymbol{\xi}) n_3(\boldsymbol{x}), \qquad k = 1, 3,$$

$$P_{m1}(\boldsymbol{x}, \boldsymbol{\xi}) = \frac{1}{2\pi} \int_\sigma e^{i\alpha_1 x_1} \Big(\frac{e^{-i\alpha_1 \xi_1}}{2C_{55}(\lambda_2^2 - \lambda_1^2)}$$

$$\times \sum_{n=1}^2 (-1)^{n+1} \Big[\Big(C_{11} n_1 i\alpha_1 - C_{55} n_3 \lambda_n \, \text{sign}(x_3 - \xi_3) \Big) B_1^{(m)}(\alpha_1, \lambda_n, x_3, \xi_3)$$

$$+ \Big(C_{55} n_3 i\alpha_1 - C_{13} n_1 \lambda_n \, \text{sign}(x_3 - \xi_3) \Big) B_3^{(m)}(\alpha_1, \lambda_n, x_3, \xi_3) \Big] e^{-\lambda_n|x_3 - \xi_3|}$$

$$+ \sum_{k=1}^4 C_k^{(m)} e^{\lambda_k x_3} \Big[\psi_1(\lambda_k) \Big(C_{11} n_1 i\alpha_1 + n_3 C_{55} \lambda_k \Big) + \psi_3(\lambda_k) \Big(C_{13} n_1 \lambda_k + C_{55} n_3 i\alpha_1 \Big) \Big] \Big) \, d\alpha_1,$$

513

$$P_{m3}(\boldsymbol{x}, \boldsymbol{\xi}) = \frac{1}{2\pi} \int_\sigma e^{i\alpha_1 x_1} \left(\frac{e^{-i\alpha_1 \xi_1}}{2C_{55}(\lambda_2^2 - \lambda_1^2)} \right.$$

$$\times \sum_{n=1}^{2} (-1)^{n+1} \left[\left(C_{13} n_3 i\alpha_1 - C_{55} n_1 \lambda_n \operatorname{sign}(x_3 - \xi_3) \right) B_1^{(m)}(\alpha_1, \lambda_n, x_3, \xi_3) \right.$$

$$+ \left. \left(C_{55} n_1 i\alpha_1 - C_{33} n_3 \lambda_n \operatorname{sign}(x_3 - \xi_3) \right) B_3^{(m)}(\alpha_1, \lambda_n, x_3, \xi_3) \right] e^{-\lambda_n |x_3 - \xi_3|}$$

$$+ \left. \sum_{k=1}^{4} C_k^{(m)} e^{\lambda_k x_3} \left[\psi_1(\lambda_k) \left(C_{55} n_1 \lambda_k + n_3 C_{13} i\alpha_1 \right) + \psi_3(\lambda_k) \left(C_{55} n_1 i\alpha_1 + C_{33} n_3 \lambda_k \right) \right] \right) d\alpha_1,$$

$$B_1^{(1)}(\alpha_1, \lambda_n, x_3, \xi_3) = (\gamma_5 \alpha_1^2 - \lambda_n^2 - k^2)/\lambda_n,$$

$$B_3^{(3)}(\alpha_1, \lambda_n, x_3, \xi_3) = (\gamma_1 \alpha_1^2 - \gamma_5 \lambda_n^2 - k^2)/\lambda_n,$$

$$B_1^{(3)}(\alpha_1, x_3, \lambda_n, \xi_3) = B_3^{(1)}(\alpha_1, x_3, \lambda_n, \xi_3) = -i\alpha_1(\gamma_5 + \gamma_7)\operatorname{sign}(x_3 - \xi_3),$$

$$\psi_1(\lambda_k) = -i\alpha_1(\gamma_7 + \gamma_5)\lambda_k, \qquad \psi_3(\lambda_k) = \gamma_5 \lambda_k^2 - \gamma_1 \alpha_1^2 + k^2.$$

Here σ is the contour in the complex plane, which is chosen in accordance with the principle of ultimate absorption and acts as a certain envelope of singularities of the integral functions [5]; being too cumbersome, the expressions for the coefficients $C_k^{(m)}$ are not given here.

In accordance with Eqs. (3) and (5), the displacement fields in the layer can be presented as a sum of two terms. The first term $u_m^*(\boldsymbol{\xi})$ is the displacement field in the medium without the defect (reference displacement field) under the action of a given load; the second term is generated by the presence of a cavity in the layer. Based on presentations (3) and (5), it is possible to calculate the displacement field everywhere in the layer, if the displacement field on the cavity boundary is found.

Two most effective methods for determining the displacement field on the cavity contour can be proposed: 1) method of integral equations and method of boundary elements based on the former, which can be used for cavities of arbitrary configurations; 2) asymptotic method for circular cavities with a small relative radius.

Method of Integral Equations. One of the most effective methods of determining the displacement fields on the cavity contour is constructing systems of boundary integral equations (BIEs) on the defect boundary l_0 on the basis of presentations (3)–(5) with allowance for the boundary conditions (2). In antiplane problem ($j = 1, 3$; $i, m = 2$) and plane problem ($i, j, m = 1, 3$), the BIE systems have the form

$$\frac{1}{2} u_m(\boldsymbol{y}) = u_m^*(\boldsymbol{y}) - \text{v.p.} \int_{l_0} \sigma_{ij}^{(m)}(\boldsymbol{x}, \boldsymbol{y}) n_j(\boldsymbol{x}) u_i(\boldsymbol{x}) \, dl_x, \qquad \boldsymbol{y} = (y_1, y_3) \in l_0. \tag{6}$$

The integral with respect to l_0 is understood in the sense of the main meaning according to Cauchy [12].

In the general case of a cylindrical cavity with an arbitrary cross-sectional shape, the BIE systems (6) were solved numerically by the boundary-element method [12, 13]. After determining the displacement fields on the cavity contour with the use of presentations (3) or (5), we calculated the field $u_m(\xi_1, h)$ ($m = 1, 2, 3$) on the layer surface $x_3 = h$.

We performed several series of numerical experiments to study the dependence of the displacement fields on the layer surface on the cavity configuration and its position and considered several cavities with arbitrary configurations [6, 11].

Figure 1 shows the real and imaginary parts of the displacement fields on the layer surface $u_1(\xi_1, h)$ and $u_3(\xi_1, h)$. The calculations were performed for austenite steel with the elastic constants $C_{11} = 2.627 \cdot 10^{11}$ N/m^2, $C_{13} = 1.45 \cdot 10^{11}$ N/m^2, $C_{33} = 2.16 \cdot 10^{11}$ N/m^2, and $C_{55} = 1.29 \cdot 10^{11}$ N/m^2.

The oscillations in the layer are excited by the normal point load applied to the point $x_0 = 0$ on the layer surface. The guide line of the cylindrical cavity l_0 is a three-petal rose ($r = 0.1 \sin 3\varphi + 0.2$) with the center at the point $(0, h/2)$, $\varkappa = kh = 2$ (one propagating mode). The number of boundary elements is $N = 60$.
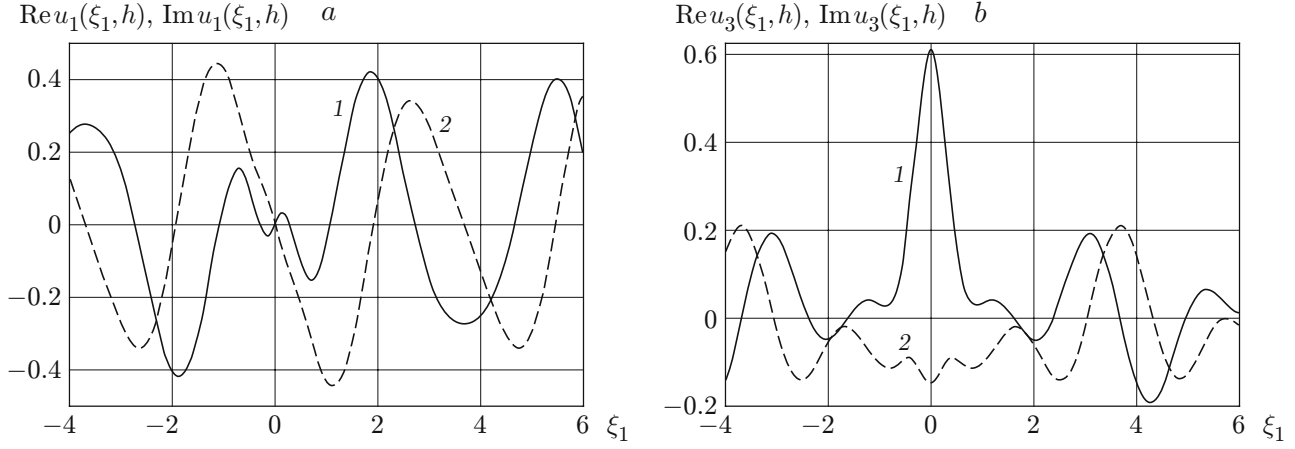
Fig. 1. Real part (curve 1) and imaginary part (curve 2) of the components of the vector of displacements on the layer surface: (a) u_1; (b) u_3.

We should also note that the procedure of solving the BIE system (6) is rather complicated and requires a significant volume of computations. Assuming that the characteristic size of the circular cavity is small, we perform an asymptotic analysis of Problem Nos. 1 and 2 with the aim of substantial simplification of wave-field calculations.

Asymptotic Method of Solving Direct Problems. The asymptotic method of solving the multiparameter problem (1), (2) on oscillations of an orthotropic layer with a cylindrical cavity whose cross-sectional shape is a circle of radius r was realized for the ranges of variation of the dimensionless parameters $\varepsilon_1 \ll 1$ and $\varepsilon_* < \varepsilon_2 < 1$, where $\varepsilon_1 = r/h$ and $\varepsilon_2 = \omega r \sqrt{\rho/C}$, with $C = C_{44}$ for Problem No. 1 and $C = C_{33}$ for Problem No. 2. The solution of the inverse problem of identification is usually constructed for $\varepsilon_2 > \varepsilon_*$, which corresponds to the case of a small defect with traveling waves in the layer.

Let us consider the asymptotic approach to solving Problem Nos. 1 and 2 by an example of Problem No. 1.

Let us study the integrand of Eq. (4). After cavity parametrization $\boldsymbol{x} = \boldsymbol{x}_0 + r\boldsymbol{\eta}$, $\boldsymbol{x}_0 = \{x_{10}, x_{30}\}$, $\boldsymbol{\eta} = \{\cos\theta, \sin\theta\}$, $\theta \in [0, 2\pi]$, we present the integrand of Eq. (4) as a sum of two terms. The first term corresponds to the static case ($\varepsilon_2 = 0$), and the second term is a certain additive to the first term:

$$K(\boldsymbol{x}_0 + r\boldsymbol{\eta}, \boldsymbol{\xi}) = K^0(\boldsymbol{x}_0 + r\boldsymbol{\eta}, \boldsymbol{\xi}) + K^1(\boldsymbol{x}_0 + r\boldsymbol{\eta}, \boldsymbol{\xi}).$$

We study the structure of the functions $K^0(\boldsymbol{x}_0 + r\boldsymbol{\eta}, \boldsymbol{\xi})$ and $K^1(\boldsymbol{x}_0 + r\boldsymbol{\eta}, \boldsymbol{\xi})$. The following estimates are obtained. If $\boldsymbol{x} \in l_0$, then $K^1(\boldsymbol{x}, \boldsymbol{\xi}) = O(\varepsilon_2^2)$ and $K^0(\boldsymbol{x}_0 + r\boldsymbol{\eta}, \boldsymbol{\xi}) = \varepsilon_1^{-1} F(\boldsymbol{x}_0, \boldsymbol{\xi}) + O(\varepsilon_1)$. Expanding the field of displacement into a series

$$u_2(\boldsymbol{x}_0 + r\boldsymbol{\eta}) = u_2^0(\boldsymbol{x}_0) + \varepsilon_1(u_{2,1}(\boldsymbol{x}_0)\cos\theta + u_{2,3}(\boldsymbol{x}_0)\sin\theta)$$

$$+ (\varepsilon_1^2/2)\Big(u_{2,11}(\boldsymbol{x}_0)\cos^2\theta + 2u_{2,13}(\boldsymbol{x}_0)\sin\theta\cos\theta + u_{2,33}(\boldsymbol{x}_0)\sin^2\theta\Big) + O(\varepsilon_1^3)$$

and substituting the resultant expansion into Eq. (3), we calculate the curvilinear integral over the defect contour. As a result, we obtain the presentation of the displacement field everywhere in the region occupied by the elastic medium:

$$u_2(\boldsymbol{\xi}) = u_2^*(\boldsymbol{\xi}) - \varepsilon_1^2 G(\boldsymbol{x}_0, \boldsymbol{\xi}) + o(\varepsilon_1^2). \tag{7}$$

Performing further the limiting transition $\boldsymbol{\xi} \to \boldsymbol{y} \in l_0$ and assuming that $\boldsymbol{y} = \boldsymbol{x}_0 + r\boldsymbol{\zeta}$, $\boldsymbol{\zeta} = \{\cos\psi, \sin\psi\}$, $\psi \in [0, 2\pi]$, we substitute the resultant expansions into Eq. (7) and equate the coefficients at the linearly independent functions 1, $\cos\psi$, $\sin\psi$, $\cos 2\psi$, and $\sin 2\psi$. Determining the expansion coefficients, we obtain an asymptotic expression for the displacement field on the cavity contour via the reference displacement field and its derivatives at the cavity center. In problem No. 1, for instance, the coefficients of expansion of the displacement field on the contour are calculated analytically; the function $G(\boldsymbol{x}_0, \boldsymbol{\xi})$ has the form

$$G(\boldsymbol{x}_0, \boldsymbol{\xi}) = \frac{\sqrt{\nu}}{2} \frac{(x_{10} - \xi_1)u_{2,1}(x_{10}, x_{30}) + (x_{30} - \xi_3)u_{2,3}(x_{10}, x_{30})}{(x_{10} - \xi_1)^2 + \nu(x_{30} - \xi_3)^2},$$

515

and the displacement field on the cavity contour is presented as

$$u_2\Big|_{l_0} = u_2^*(\boldsymbol{x}_0) + \varepsilon_1\Big(u_{2,1}^*(\boldsymbol{x}_0)(\sqrt{\nu}+1)\cos\theta + u_{2,3}^*(\boldsymbol{x}_0)\frac{\sqrt{\nu}+1}{\sqrt{\nu}}\sin\theta\Big)$$

$$+\frac{\varepsilon_1^2}{2}\Big(\frac{u_{2,11}^*(\boldsymbol{x}_0)(\nu+\sqrt{\nu}+1)-\sqrt{\nu}u_{2,33}^*(\boldsymbol{x}_0)}{\nu+1}\cos^2\theta + u_{2,13}^*(\boldsymbol{x}_0)\frac{(\sqrt{\nu}+1)^2}{\sqrt{\nu}(\sqrt{\nu}+2)}\sin 2\theta$$

$$+\frac{-\sqrt{\nu}\,u_{2,11}^*(\boldsymbol{x}_0)+u_{2,33}^*(\boldsymbol{x}_0)(\nu+\sqrt{\nu}+1)}{\nu+1}\sin^2\theta\Big)+O(\varepsilon_1^2).$$

Thus, in Problem No. 1, we obtained an explicit presentation of the displacement field on the contour without using the procedure of discretization of BIE (6) on the basis of the boundary-element method.

Based on relation (3), we can construct a presentation of the displacement field in the zone far from the defect ($\xi_1 > x_{10}$) on the layer surface $x_3 = h$. Calculating the contour integral in Eq. (3) with the use of the theory of residues and separating the amplitudes of the displacement field on the upper boundary in the far zone, we obtain a formula for convenient calculations of the wave field in Problem No. 1:

$$u_2(\xi_1,h) = u_2^*(\xi_1,h) - \sum_{p=1}^{M} A_p(\boldsymbol{x}_0,r)\,\mathrm{e}^{i\alpha_p\xi_1} + O(\mathrm{e}^{-\gamma\xi_1}). \tag{8}$$

The set of the poles $\{\alpha_n,\, n=1,2,\ldots\}$ consists of a countable set of purely imaginary poles and a finite number M of real poles. The real poles α_n correspond to traveling waves in the layer, and the remaining poles characterize nonuniform modes whose amplitude exponentially decrease.

Within the framework of the proposed asymptotic approach, the expressions for the amplitudes of the modes propagating in the layer have the form

$$A_p(\boldsymbol{x}_0,r) = (-1)^{p+1}r^2\pi\,\mathrm{e}^{-i\alpha_p x_{10}}\Big[k^2u_2^*(\boldsymbol{x}_0)\sinh\,(\lambda_p x_{30})/(\nu\alpha_p)$$

$$+ iu_{2,1}^*(\boldsymbol{x}_0)\sinh\,(\lambda_p x_{30}) - u_{2,3}^*(\boldsymbol{x}_0)\lambda_p\cosh\,(\lambda_p x_{30})/(\nu\alpha_p)\Big], \tag{9}$$

where

$$\alpha_p = \sqrt{k^2h^2 - \pi^2(-0.5+p)^2}/(h\sqrt{\nu}), \quad \lambda_p = i\pi(-0.5+p)/h, \quad p=1,2,\ldots,M.$$

We also note that all information about the defect configuration is contained in the expression for the traveling wave amplitudes (9); therefore, the presentation for calculating the field on the layer surface (8) will be further used to solve the inverse problem of defect identification.

A number of numerical experiments on calculating the wave fields on the layer surface were performed for the case of a cylindrical cavity with a round cross section of a small relative size. The study involved three approaches [8, 9]: boundary-element method, asymptotic approach, and Born approximation used in acoustics [3]. The area of applicability of the asymptotic approach and the Born approximation was determined in calculating the wave fields in the far zone $\varepsilon_1 = 0.001$–0.300 at $\varepsilon_2 < 1$.

Formulation and Solution of Inverse Problems. The solution of inverse problems of reconstruction of cavity parameters in the case of antiplane and plane oscillations of the layer is constructed on the basis of solving direct problems and some information about the displacement field on its surface. Constructing the solution of such inverse problems is reduced to solving a complicated nonlinear system of integral equations with respect to displacements on the cavity contour and the contour itself [1, 11]. This solution is obtained by a certain iterative process with the initial approximation being found by the method of regularization on compact sets. In this approach, the sought contour is usually determined in the class of the simplest configurations (circumference or ellipse) [6, 8, 9, 11]. In the present work, the sought contour is determined in a wider class of contours. For this purpose, the radius vector defining the cavity contour in the polar coordinate system is expanded into the Fourier series with a finite number of harmonics retained. Thus, the problem solution is reduced to determining the coefficients of the Fourier series a_i ($i=0,1,2,3$) and b_j ($j=1,2,3$) and the coordinates of the cavity center. The unknown parameters are found from the condition of the minimum value of the non-quadratic residue functional constructed by the method of positional probing:
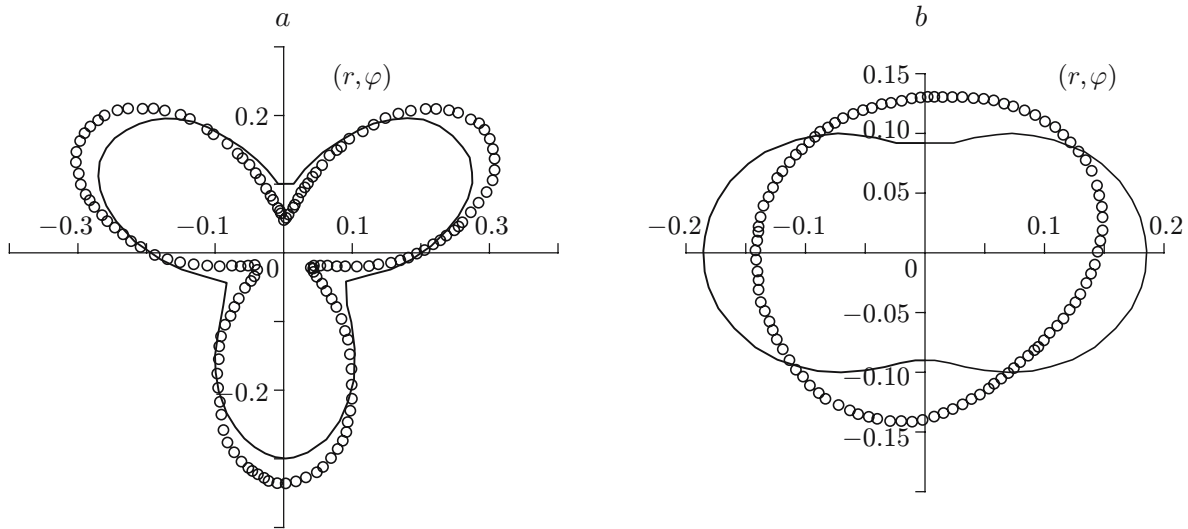
516

Fig. 2. Sought contour (solid curve) and reconstructed contour (points) of the cavity: (a) three-petal rose; (b) ellipse.

$$\Phi(\boldsymbol{z}) = \sum_m \sum_{k=1}^{N_*} |f_m(\xi_{1k}) - u_m(\boldsymbol{z}, \xi_{1k})|^2,$$

$$\xi_{1k} \in [c, d], \quad m = 1, 2, 3, \quad \boldsymbol{z} = \{a_i, b_j, x_{10}, x_{30}\}, \quad i = 0, 1, 2, 3, \quad j = 1, 2, 3.$$

A number of numerical experiments were performed for reconstruction of the contours of an arbitrary configuration in a nine-dimensional Euclidean space. The minimum of the residue functional was determined on the basis of the genetic algorithm [14]. Figure 2 illustrates the sought contour (solid curve) and reconstructed contour (points) of the cavity. Figure 2a shows the result of reconstruction of the contour of a cylindrical cavity l_0 ($r = 0.1 \sin 3\varphi + 0.2$) with the center at the point $(0, h/2)$, and Fig. 2b shows the result of reconstruction of the contour l_0 — an ellipse with semiaxes $a = 0.2$ and $b = 0.1$ and with the center at the point $(0, h/2)$. The parameter $\varkappa = kh = 3.7$ corresponds to three traveling waves, the number of boundary elements is $N = 32$, and the number of probing points is $N_* = 6$.

Note that the iterative procedure of searching for the minimum of the residue functional is rather expensive in terms of time, because the corresponding direct problem is solved at each step. The proposed algorithm of the solution, however, can be substantially simplified by using the assumption about a small relative size of the defect. In this case, the defect contour is assumed to be determined by the asymptotic approach in the class of circumferences.

Let prescribed amplitude values A_p^* ($p = 1, 2$) of the displacement field in the far zone on the upper boundary of the layer be used as additional information for Problem No. 1. With the use of the expressions for the amplitudes (9), solving of the problem of cavity identification can be reduced to determining its parameters step by step. We involve into consideration the residue functionals

$$\Phi(x_{10}, x_{30}) = \left| \frac{A_1^*}{A_2^*}(k) - \frac{A_1(x_{10}, x_{30}, k)}{A_2(x_{10}, x_{30}, k)} \right|^2; \tag{10}$$

$$\Phi(r) = \sum_{p=1}^{2} |A_p^*(k) - A_p(r, k)|^2. \tag{11}$$

After minimization of functional (10), the found values of x_{10} and x_{30} were substituted into functional (11), and minimization of the latter was performed to find the radius. A number of numerical experiments were performed on reconstruction of the contour of defects of a small relative size (circumference, ellipse [8, 9], and three-petal rose) with the use of the asymptotic approach. The results of the numerical experiments on reconstruction of the contours of arbitrary configurations in the class of circumferences are summarized in Table 1.

517

TABLE 1

Results of Numerical Experiments on Reconstruction of Cavity Parameters

True parameters of the cavity	Reconstructed parameters of the cavity
Ellipse: $a = 0.02$, $b = 0.01$, $\psi = \pi/6$, $x_{10} = 1$, and $x_{30} = 0.5$	$r = 0.0149$, $x_{10} = 1.044$, and $x_{30} = 0.477$
Ellipse: $a = 0.025$, $b = 0.01$, $\psi = 0$, $x_{10} = 1$, and $x_{30} = 0.5$	$r = 0.01532$, $x_{10} = 0.991$, and $x_{30} = 0.498$
Three-petal rose: $r = 0.015 \sin 3\varphi + 0.04$, $x_{10} = 1$, and $x_{30} = 0.6$	$r = 0.0427$, $x_{10} = 0.974$, and $x_{30} = 0.613$
Three-petal rose: $r = 0.015 \sin 3\varphi + 0.04$, $x_{10} = 1$, and $x_{30} = 0.85$	$r = 0.0436$, $x_{10} = 1.053$, and $x_{30} = 0.899$

Note. ψ is the angle of inclination of the ellipse to the Ox_1 axis.

Note that the relative difference in the areas of the reconstructed and sought cross sections of the cavity was smaller than 5% for defects located at a medium depth and 11% for subsurface defects. The coordinates of the cavity center were found with a relative error smaller than 6%. Thus, the proposed algorithm offers a fairly accurate estimate of the defect scale and its position in the layer.

An analysis of numerical experiments performed with the use of the asymptotic approach for solving inverse problems in the case of a defect with an arbitrary configuration of a small relative size allows us to conclude that the proposed algorithm of defect identification is rather effective and allows the time of reconstruction of defect parameters to be substantially reduced.

REFERENCES

1. A. O. Vatul'yan, *Inverse Problems in Mechanics of Deformable Solids* [in Russian], Fizmatlit, Moscow (2007).
2. H. Henl, A. W. Maue, and K. Westpfahl, *Theorie der Beugung*, Springer, Berlin (1961).
3. A. A. Goryunov and A. V. Saskovets, *Inverse Problems of Scattering in Acoustics* [in Russian], Izd. Mosk. Univ., Moscow (1989).
4. M. Bonnet and A. Constantinescu, "Inverse problems in elasticity," *Inverse Probl.*, No. 21, 1–50 (2005).
5. I. I. Vorovich and V. A. Babeshko, *Dynamic Mixed Problems of the Elasticity Theory for Nonclassical Areas* [in Russian], Nauka, Moscow (1979).
6. A. O. Vatul'yan and O. A. Suvorova, "Inverse problem for an elastic layer with a cavity," *Ékolog. Vestn. Nauch. Tsentr. Chernomor. Sotrudnichestva*, No. 1, 10–16 (2005).
7. A. O. Vatul'yan and A. Ya. Katsevich, "Vibrations of an elastic orthotropic layer with a cavity," *J. Appl. Mech. Tech. Phys.*, **32**, No. 1, 90–93 (1991).
8. A. O. Vatul'yan and O. A. Belyak, "Reconstruction of small cavities in an elastic layer," *Defektoskopiya*, No. 10, 33–39 (2006).
9. A. O. Vatul'yan and O. A. Belyak, "Asymptotic approach to solving an inverse problem on reconstruction of a cavity in an elastic layer," *Vestn. Donets. Univ., Ser. A: Estestv. Nauki*, No. 1, 73–79 (2006).
10. A. O. Vatul'yan, I. A. Guseva, and I. M. Sinyakova, "Fundamental solutions for an orthotropic medium and their applications," *Izv. Sev.-Kavk. Nauch. Tsentra, Ser. Estestv. Nauki*, No. 2, 81–85 (1989).
11. O. A. Belyak and I. V. Baranov, "Inverse problem for a layer with a cavity," in: *Advanced Problems of Mechanics of Continuous Media*, Proc. 10th Int. Conf. (Rostov-on-Don, December 5–9, 2006), Valeology Centers in Higher Educational Institutions of Russian, Rostov-on-Don (2006), pp. 56–61.
12. C. Brebbia, J. Telles, and L. Wrobel, *Boundary Element Techniques*, Springer, Heidelberg (1984).
13. P. Banerjee and R. Butterfield, *Boundary Element Methods in Engineering Science*, McGraw-Hill, London (1981).
14. I. V. Baranov, A. O. Vatul'yan, and A. N. Solov'ev, "One genetic algorithm and its application in inverse problems of identification of elastic media," *Vychisl. Tekhnol.*, No. 3, 14–26 (2006).